


# Gene and Allele-Specific Expression Underlying the Electric Signal Divergence in African Weakly Electric Fish

Feng Cheng,<sup>1</sup> Alice B. Dennis,<sup>1,2</sup> Otto Baumann,<sup>3</sup> Frank Kirschbaum,<sup>1,4</sup> Salim Abdelilah-Seyfried,<sup>3</sup> and Ralph Tiedemann <sup>1,\*</sup>

<sup>1</sup>Unit of Evolutionary Biology/Systematic Zoology, Institute of Biochemistry and Biology, University of Potsdam, Potsdam, Germany

<sup>2</sup>Laboratory of Adaptive Evolution and Genomics, Research Unit of Environmental and Evolutionary Biology, Institute of Life, Earth & Environment, University of Namur, Namur, Belgium

<sup>3</sup>Department of Animal Physiology, Institute of Biochemistry and Biology, University of Potsdam, Potsdam, Germany

<sup>4</sup>Department of Crop and Animal Science, Faculty of Life Sciences, Humboldt University, Berlin, Germany

\*Corresponding author: E-mail: tiedeman@uni-potsdam.de.

Associate editor: Sophie von der Heyden

## Abstract

In the African weakly electric fish genus *Campylomormyrus*, electric organ discharge signals are strikingly different in shape and duration among closely related species, contribute to prezygotic isolation, and may have triggered an adaptive radiation. We performed mRNA sequencing on electric organs and skeletal muscles (from which the electric organs derive) from 3 species with short (0.4 ms), medium (5 ms), and long (40 ms) electric organ discharges and 2 different cross-species hybrids. We identified 1,444 upregulated genes in electric organ shared by all 5 species/hybrid cohorts, rendering them candidate genes for electric organ-specific properties in *Campylomormyrus*. We further identified several candidate genes, including *KCNJ2* and *KLF5*, and their upregulation may contribute to increased electric organ discharge duration. Hybrids between a short (*Campylomormyrus compressirostris*) and a long (*Campylomormyrus rhynchophorus*) discharging species exhibit electric organ discharges of intermediate duration and showed imbalanced expression of *KCNJ2* alleles, pointing toward a *cis*-regulatory difference at this locus, relative to electric organ discharge duration. *KLF5* is a transcription factor potentially balancing potassium channel gene expression, a crucial process for the formation of an electric organ discharge. Unraveling the genetic basis of the species-specific modulation of the electric organ discharge in *Campylomormyrus* is crucial for understanding the adaptive radiation of this emerging model taxon of ecological (perhaps even sympatric) speciation.

**Key words:** African weakly electric fish, electric organ discharge, adaptive radiation, potassium channel, gene expression, allele-specific expression.

## Introduction

Electric fish have independently evolved 6 times (Darwin 1859; Bass 1986; Kirschbaum and Formicki 2020). They possess a specific myogenic electric organ (EO) derived from skeletal muscle (SM) fibers except for Apterontidae, which possess an EO derived from nervous tissue (Smith 2013). Comparative genomics have unraveled this convergent phenotypic evolution to originate in part also from convergence on the molecular level: both voltage-dependent sodium and potassium channels are involved in the EO development and physiology. Because of the teleost-specific whole genome duplication (Glasauer and Neuhauss 2014), these fish possess 2 copies of most genes and subfunctionalization among paralogs and differential expression between EO and SM seem to play a major role in the transition of myocytes to electrocytes. A prominent example is the voltage-gated sodium ( $Na_v$ ) channel

gene (*SCN4a*): convergently in 3 electrogenic taxa (Mormyridae, Siluriformes, and Gymnotiformes), only 1 paralog (*SCN4ab*) is still expressed in SM, but the other 1 (*SCN4aa*) is exclusively expressed in the EO, indicating a crucial role for electrogenesis (Zakon 2012; Wang and Yang 2021; LaPotin et al. 2022). The  $Na_v$  channel gene (*SCN4aa*) is regulated by *FGF13a* in the 3 electric fish lineages Siluriformes, Gymnotiformes, and Mormyridae (Gallant et al. 2014). Differential expression of multiple isoforms of  $\alpha$ - and  $\beta$ -subunits of sodium/potassium ATPase is important in the EO as well (Gallant et al. 2012, 2014; Lamanna et al. 2015). In addition, several transcription factors, *HEY1*, *MEF2a*, and *SIX2a*, are convergently upregulated in the EOs of those electric fish lineages (Kim et al. 2004; Gallant et al. 2012, 2014). EOs hence comprise a prime example of convergent evolution in both genotype and phenotype.

Received: October 31, 2023. Revised: December 15, 2023. Accepted: January 29, 2024

© The Author(s) 2024. Published by Oxford University Press on behalf of Society for Molecular Biology and Evolution.

This is an Open Access article distributed under the terms of the Creative Commons Attribution License (<https://creativecommons.org/licenses/by/4.0/>), which permits unrestricted reuse, distribution, and reproduction in any medium, provided the original work is properly cited.

Open Access

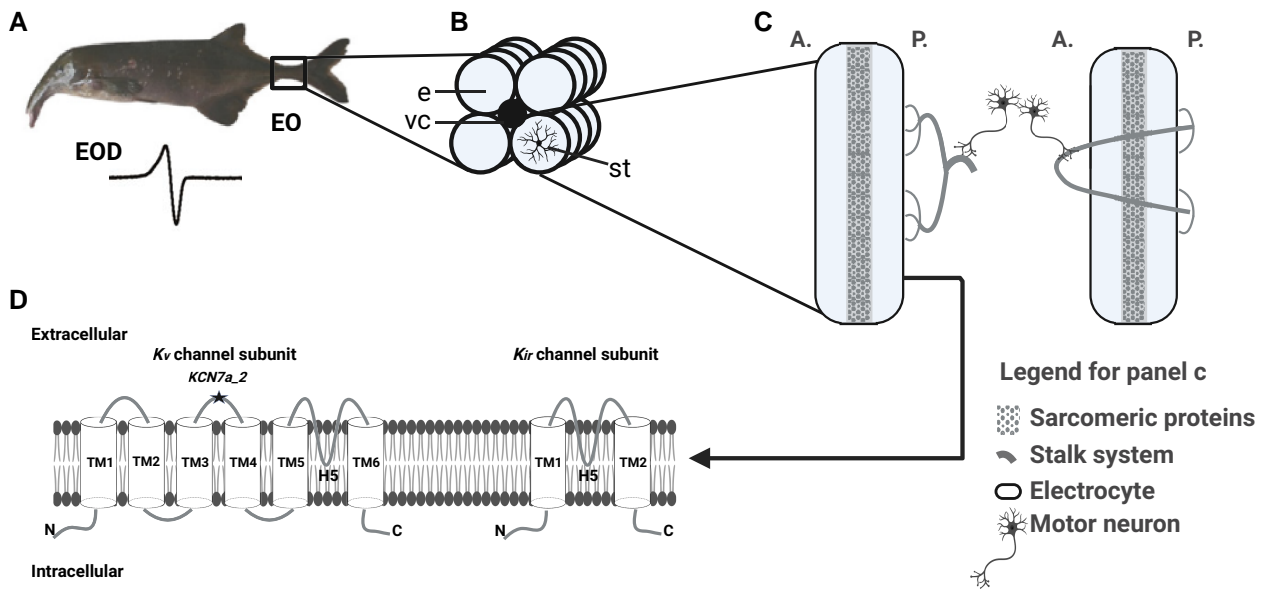


**Fig. 1.** EO and electrocyte structure in *Campylomormyrus* and schematic illustration for potassium channels. a) Electric organ (EO) and electric organ discharge (EOD) in an adult *Campylomormyrus* fish. b) The EO consists of four columns of electrocytes (e) which surround the vertebral column (vc), the stalk system (st) is connected to the posterior face of the electrocyte. c) Anterior (A.) and posterior (P.) faces of electrocytes with two types of stalk system. Panel c is modified from Gallant et al. (2012). d) Schematic illustration of voltage-gated potassium ( $K_v$ ) channel and inwardly rectifying ( $K_{ir}$ ) channel subunit.  $K_v$  channel subunit contains six transmembrane (TM) helices, a pore-forming (H5) loop, and cytosolic NH<sub>2</sub> (N) and COOH (C) termini. The gene KCN7A\_2 was inferred to be under positive selection and the mutation encodes the loop between TM3-4.  $K_{ir}$  channel subunit contains only two TMs.

One of the electric fish clades, mormyrid fish, contains about 200 described species that are endemic to Africa. This outstanding adaptive radiation within the otherwise species-poor basal lineage of osteoglossiforms is putatively due to their species-specific weak electric signals, which are used for both electrolocation and electrocommunication (Feulner et al. 2009a, b). Divergence in EO discharge (EOD) is considered a major driver in the ecological (and possibly sympatric) speciation in the mormyrid genus *Campylomormyrus*, which is mainly distributed in the Congo River (Tiedemann et al. 2010).

The genus *Campylomormyrus* comprises 15 described species, which have profoundly diverged in their EOD with regard to signal duration and waveform (Feulner et al. 2009a). Those species possess either long or short, bi-phasic or triphasic, but always species-specific EODs that function as a prezygotic reproductive isolation mechanism and are supposed to have arisen via divergent selection among closely related species (Feulner et al. 2009a). In adult *Campylomormyrus*, the EO, confined to the caudal peduncle (Fig. 1a), is composed of specialized electrocytes (Paul et al. 2015). They have a flat, disk-shaped appearance with a clear orientation toward the longitudinal body axis (Fig. 1b). Unlike SM myocytes, electrocytes possess a number of special evaginations, called stalks, mostly on the posterior face (Paul et al. 2015). These stalks are either fused into major stalks on the posterior face (Fig. 1c, left) or they penetrate the electrocyte and merge at the anterior face to constitute to major stalks (Fig. 1c, right). A branch of the spinal nerve forms numerous synapses with the major stalk, whether on the posterior or on the anterior face

of the electrocyte, and the action potentials are propagated along the stalk system to the disk-like part of the electrocyte (Paul et al. 2015). The externally measurable EOD is formed by simultaneous action potentials of all electrocytes. The shape of the EOD in *Campylomormyrus* is often associated with the penetration of the stalks (Gallant et al. 2011), while the structural basis of the EOD duration, which can vary 100-fold across species, is still only partially understood. A very elongated EOD (~40 ms) is produced by *Campylomormyrus rhynchophorus* and *Campylomormyrus numenius*, which exhibit large foldings or evaginations on the anterior face of the electrocytes, so-called papillae (Kirschbaum et al. 2016; Korniienko et al. 2021). In 2 species with relatively short EOD (Fig. 2a), *Campylomormyrus compressirostris* (0.4 ms) and *Campylomormyrus tamandua* (0.4 ms), many small stalks fuse into 1 major stalk of large diameter after their origin (Paul et al. 2015). In contrast, the stalk system in species with an EOD of medium (e.g. *Campylomormyrus tshokwe*, 5 ms) or long duration (e.g. *C. numenius*, 40 ms) is more branched (Paul et al. 2015). Apart from these differences in the stalk system, species with highly diverged EOD waveforms still show similar electrocyte geometry suggesting further core mechanisms to contribute to the observed EOD variations. Since the electrocytes generate action potentials for EOD, the distribution and repertoire of ion currents have long been considered to play a key role in EOD formation (Lamanna et al. 2014, 2015; Paul et al. 2016; Nagel et al. 2017; Swapna et al. 2018).

Sodium and potassium fluxes are considered the most important ion currents in controlling the EOD (Stoddard

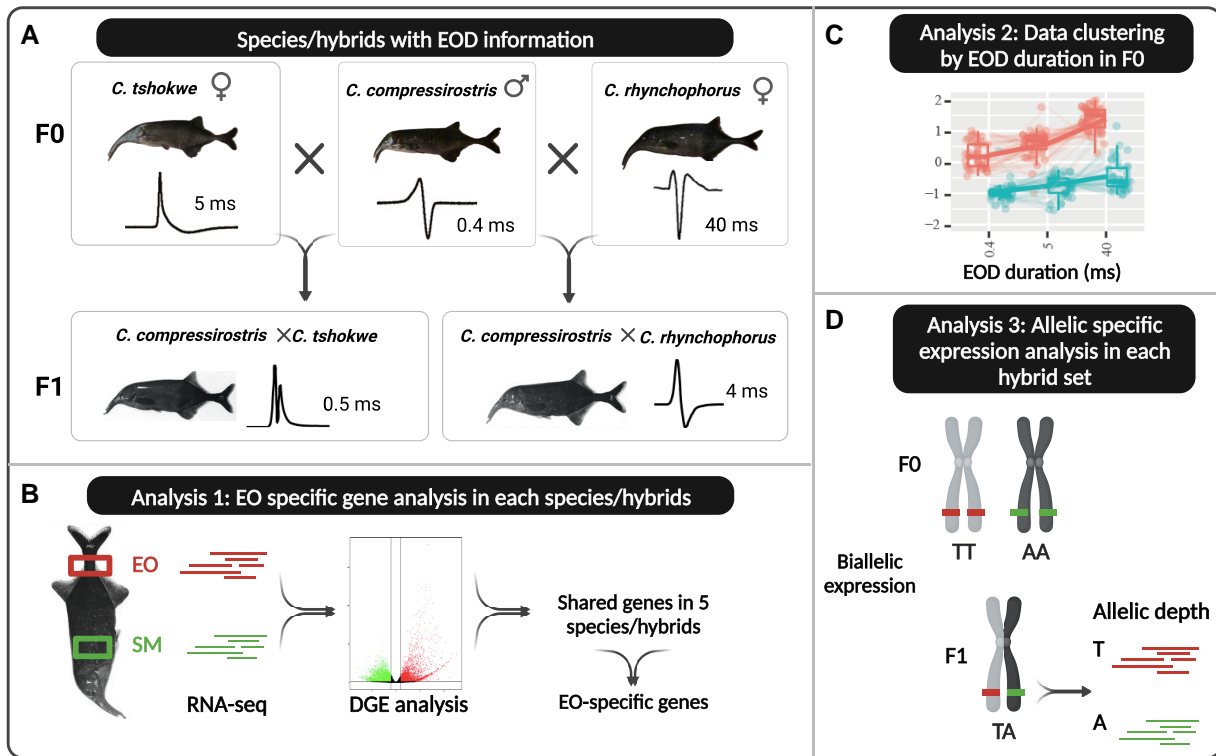


**Fig. 2.** EOD shape and duration of *Campylomormyrus* species and hybrids and the working flow of this study. a) Species/hybrids samples used in the study and their EOD pattern. b) Differential gene expression (DGE) analysis between electric organ (EO) and skeletal muscle (SM) for each species/hybrid to identify genes with EO-specific expression. c) RNA-seq data clustering based on EOD duration change for EO (red) and SM (blue) in F0 species. d) Allele specific expression analysis in each hybrid set.

and Markham 2008). They are the basic requirements for generating an action potential (Mehaffey et al. 2006). Consequently, abundance and properties of sodium and potassium channels are likely to profoundly influence the EOD. The potassium channels can be classified into different classes based on their structure and function: voltage-gated ( $K_v$ , includes subfamilies, e.g. *shaker*-related *KCNA* and *shab*-related *KCNB*), inwardly rectifying ( $K_{ir}$ ), tandem pore domain channels ( $K_{2p}$ ), ligand-gated channels, and calcium-activated channels ( $K_{ca}$ ) (Kuang et al. 2015). Two paralogs of the *KCNA7* channel gene originate from the whole genome duplication event in teleost fish, and these paralogs might have undergone subfunctionalization or neofunctionalization in mormyrids: one of them *KCNA7a* is predominantly expressed in the EO of mormyrids, while *KCNA7b* is preferentially expressed in SM (Swapna et al. 2018). The  $K_v$  channel contains 6 transmembrane helices (Fig. 1d). In *KCNA7a*, a nonsynonymous substitution was observed in the transmembrane helix 3 and 4 linkers and the encoded amino acid substitution might relate to the EOD duration difference among the mormyrid taxa *Brienomyrus* and *Gymnarchus* (Swapna et al. 2018).

This study focuses on potential molecular mechanisms underlying the divergent EOD among *Campylomormyrus* species as a potential major driver of their adaptive radiation. This study takes further advantage of artificially bred hybrid electric fish. *Campylomormyrus* species

hybrids often exhibit an adult EOD, which is similar to the juvenile EOD from one of the parental species, and the adult EOD duration in hybrids is usually intermediate between the 2 parental species (Kirschbaum et al. 2016). Gene expression analyses in hybrids further enable assessment of allelic-specific expression, relative to the expressed trait of interest (here, EOD duration). To enhance our understanding of the genetic regulation of EOD divergence among *Campylomormyrus* species, especially for the EOD duration divergence, we (i) compared the gene expression pattern between EO and SM in the 3 F0 species, *C. compressirostris* (*com*, short and biphasic EOD), *C. tshokwe* (*tsh*, medium and biphasic EOD), and *C. rhynchophorus* (*rhy*, long and triphasic EOD), and 2 F1 hybrids, *C. compressirostris* ♂ × *C. tshokwe* ♀ (*com* × *tsh*, short and biphasic EOD) and *C. compressirostris* ♂ × *C. rhynchophorus* ♀ (*com* × *rhy*, medium and biphasic EOD); (ii) clustered RNA-seq data relative to the EOD duration in 3 F0 species to infer genes with duration-specific expression; and (iii) assessed biallelic-specific expression for 2 hybrid sets (each set includes 2 F0 parental species and their hybrid; Fig. 2).

## Results

We examined overall patterns in gene expression using a principal component analysis (PCA) based on all expressed genes (Fig. 3a). Expression profiles of SMs and EOs were

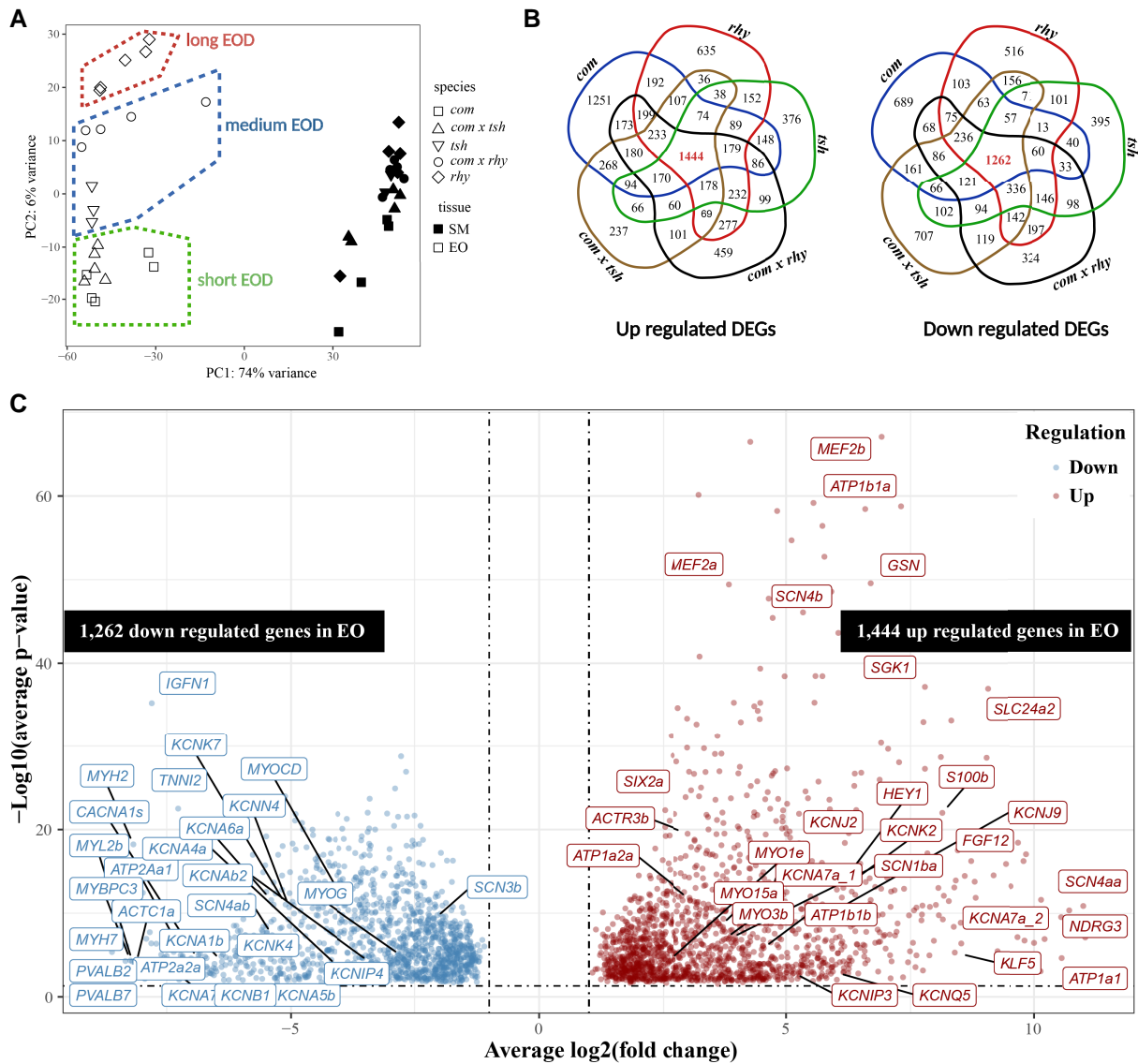


**Fig. 3.** Differential gene expression between EO and SM in *C. compressirostris* (*com*), *C. rhynchophorus* (*rhy*), *C. tshokwe* (*tsh*), and hybrids *C. compressirostris* ♂ × *C. rhynchophorus* ♀ (*com* × *rhy*) and *C. compressirostris* ♂ × *C. tshokwe* ♀ (*com* × *tsh*). a) Principal component analysis (PCA) of gene expression levels between EO and SM in 5 species/hybrids. b) Venn Diagram graph for up (left) and down (right) regulated genes shared in 5 species/hybrids. All differentially expressed genes (DEGs) have  $|\log_2(\text{fold change})| > 1$  and a  $p$ -value  $< 0.05$ . Many of the DEGs are related to “membrane” and “plasma membrane” (see [supplementary fig. S1](#)). c) Volcano plot showing genes differentially expressed in EO (relative to SM) in all 5 species/hybrids. X-axis is the average  $\log_2(\text{fold change})$  among 5 species/hybrids, and y-axis is the associated  $-\log_{10}(\text{average } p\text{-value for 5 species/hybrids})$ . Potential candidate genes and genes with low  $p$ -value or high fold change are labeled with their name.

broadly separated along PC1, which explained 74% of variance. The SMs’ expression profiles from all species/hybrids clustered together; however, species/hybrid-specific EOs’ expression profiles were stratified along PC2 (explained 6% of variance), relative to EOD duration (Fig. 3a). The PCA hence indicates that gene expression in *Campylomormyrus* (i) is EO specific, compared with SM, and (ii) relates to EOD duration, enabling inference of underlying candidate genes.

### Genes with EO-Specific Expression Pattern

Differential gene expression analysis was used for pairwise comparisons between EO and SM for each species and

hybrid (Fig. 2b). We identified significantly differentially expressed genes (DEGs) based on a  $|\log_2(\text{fold change})| > 1$  and a  $P < 0.05$ . We specifically identified genes with an EO-specific expression pattern shared among all *Campylomormyrus* species/hybrids. There were 1,444 up-regulated and 1,262 down-regulated DEGs that were shared in the comparison of EO and SM in all species/hybrids (Fig. 3b and c).

Among the DEGs upregulated in the EO, 54 genes were related to transmembrane ion transport (Fig. 3c and Table 1; [supplementary table S1, Supplementary Material online](#)). We identified 4 genes encoding sodium/potassium-ATPase  $\alpha$ - and  $\beta$ -subunit (*ATP1a1*, *ATP1a2a*,

*ATP1b1a*, and *ATP1b1b*) and 3  $Na_v$  channel genes (*SCN4aa*, *SCN4b*, and *SCN1ba*). Several genes encoding for different types of potassium channels were also identified: 4  $K_v$  channel genes (*KCNA7a\_1*, *KCNA7a\_2*, *KCNIP3*, and *KCNQ5*), 2  $K_{ir}$  channel genes (*KCNJ2* and *KCNJ9*), and 1  $K_{2p}$  channel gene (*KCNK2*). Further transmembrane ion transport DEGs were chloride, calcium, and other cation channel genes (supplementary table S1, Supplementary Material online). Several solute carrier family genes were also upregulated in the EO, in particular *SLC24a2* (Table 1).

Eighteen genes upregulated in the EO were associated with cytoskeletal and sarcomeric protein (supplementary table S1, Supplementary Material online). The predicted functions of those genes were mainly related to F-actin dynamics and unconventional myosin activity (Table 1). A signaling gene *NDRG3* showed very high overexpression in EO ( $\log_2FC = 11.02$ ), as well as the genes *SGK2*, *S100b*, and *FGF12*. The upregulated transcription factors in the EO included Krüppel-like factor 5 (*KLF5*), *FOXL2*, *SIX2a*, *HEY1*, and 2 myocyte-specific enhancer factors (*MEF2a* and *MEF2b*).

In the downregulated DEGs in EO (or upregulated in SM), 44 genes were classified into the category “cytoskeletal and sarcomeric” (Fig. 3c; supplementary table S2, Supplementary Material online). There were 37 transmembrane ion transport genes downregulated in EO, which were related to the ions potassium, sodium, and calcium. In contrast to the expression pattern of the 2 *KCNA7a* copies, 5  $K_v1$  subfamily genes (*KCNA1b*, *KCNA4a*, *KCNA5b*, *KCNA6a*, and *KCNA7b*) were downregulated in the EO. This was also the case for other potassium and sodium channel genes, e.g.  $K_v$  subfamily genes (*KCNB1*, *KCNE4*, and *KCNIP4*),  $K_{2p}$  subfamily genes (*KCNK4*, *KCNK7*), a  $K_{ca}$  subfamily gene (*KCNN4*), and  $Na_v$  channel genes (*SCN3b*, *SCN4ab*). Two muscle-specific transcription factors, *MYOCD* and *MYOG*, were also downregulated in EO (supplementary table S2, Supplementary Material online).

We applied a Gene Ontology (GO) enrichment analysis to further examine the function of all the up- and down-regulated DEGs in EO, respectively (Dennis et al. 2003). Among the upregulated DEGs in the EO, there were 44 significantly enriched GO terms (Fisher’s exact test  $P < 0.01$ ; supplementary fig. S1 and table S3, Supplementary Material online). Among them, the 3 GO terms with the highest number of DEGs were all related to the cell membrane: membrane (464 DEGs), integral component of membrane (309 DEGs), and plasma membrane (237 DEGs). There were 47 DEGs assigned to the enriched GO term “ion transport.” Sixty-two and 35 DEGs were assigned to the enriched Golgi-related GO terms “Golgi membrane” and “Golgi apparatus,” respectively. In addition, there were 23 DEGs assigned to the enriched GO term “actin filament binding.” There were 73 GO terms significantly enriched for DEGs downregulated in the EO (upregulated in SM; supplementary fig. S2 and table S4, Supplementary Material online). They were associated with skeletal and cardiac muscle tissue-related GO terms.

## Genes with Expression Levels Related to EOD Duration

The PCA plot from transcriptome-wide gene expression showed a significant association between overall gene expression and EOD duration in all species/hybrids (PC2 in Fig. 3a; accounting for 6% of the variance in gene expression). DESeq2 provides a likelihood ratio test (LRT) that compares how well a gene’s read count data fit a “full model” (with independent variables) compared to a “reduced model” (without those variables). Therefore, it is well suited to explore whether there are any significant associations of gene expression levels across a series of values of an independent variable (here, EOD duration; Love et al. 2015). Specifically, we used this approach to test whether a gene’s expression fits a pattern of increasing or decreasing over the different durations in 2 different tissues, EO and SM (Bendjilali et al. 2017). In order to avoid any bias potentially stemming from distorted expression pattern in the hybrids, we only used the quantification data from the parental purebred (F0) species. The LRT analysis returned 1,874 significant genes using a threshold of adjusted  $P$ -value ( $P_{adj}$ )  $< 0.05$ . Those genes were further sorted into groups using the *degPatterns* function (Pantano 2019). Each such group contained genes following a specific pattern of expression across the different duration values in the analyzed tissues EO and SM (Pantano 2019).

The *degPatterns* function generated 27 groups of different expression patterns in EO and SM, relative to EOD duration (supplementary fig. S3, Supplementary Material online). To identify EOD duration-specific genes, we focused on the groups meeting the following criteria: (i) the gene expression level in EO is higher than SM in all F0 species (i.e. the gene is consistently upregulated in the EO), and (ii) the gene expression level in the EO shows an increasing or decreasing pattern, relative to EOD duration. Two groups showed a consistent increasing expression pattern (group 5, 41 genes; group 6, 239 genes) and 1 a decreasing expression pattern (group 3, 405 genes), relative to the EOD duration (Fig. 4).

In the increased expression pattern groups (5 and 6), we found  $K_{ir}$  subfamily gene *KCNJ2* and the transcription factor *KLF5*; both were found among the genes with EO-specific expression as well (Table 2). In the decreased expression group 3, there were 2 transmembrane ion transport genes (*KCNK6* and *KCNQ5*) and 2 cytoskeletal and sarcomeric genes (*ACTR3b* and *NHS*; Table 2).

Assigning DEGs with increasing expression pattern to GO terms revealed 19 significantly enriched (Fisher’s exact  $P < 0.05$ ) GO terms (supplementary fig. S4 and table S5, Supplementary Material online). Eighteen genes were assigned to the enriched GO term “Golgi apparatus” and 13 to “ion transport.” Among the genes with decreasing expression pattern (group 3), 41 GO terms were significantly enriched (supplementary fig. S5 and table S6, Supplementary Material online). Twelve of the genes were assigned to the GO term “axon guidance,” which yielded the lowest  $P$ -value. There were also several enriched terms that might be functionally related to the

**Table 1** Candidate genes in EO and their descriptions, including the average log<sub>2</sub>FC and average P-value

ID	Blast gene	Highlights of predicted function	Gene description	Category	Average log <sub>2</sub> FC	Average P-value
maker-ptg0003611-augustus-gene-0.2-mRNA-1	ACTR3b	F-actin dynamics/polymerization	ARP3 actin-related protein 3 homolog B	Cytoskeletal and sarcomeric	3.02	3.16E-20
maker-ptg0003461-snap-gene-25.173-mRNA-1	GSN	F-actin dynamics/polymerization	Gelsolin	Cytoskeletal and sarcomeric	6.70	2.7189E-50
snap_masked-ptg0000281-processed-gene-137.57-mRNA-1	MYO15a	Unconventional myosin; actin-based motor protein	Unconventional myosin-XV	Cytoskeletal and sarcomeric	3.68	3.4002E-09
maker-ptg0010031-snap-gene-2.16-mRNA-1	MYO1e	Unconventional myosin; actin-based motor protein	Unconventional myosin-le	Cytoskeletal and sarcomeric	2.63	5.7074E-05
maker-ptg0020901-augustus-gene-35.16-mRNA-1	MYO3b	Unconventional myosin; actin-based motor protein	Myosin-IIIb	Cytoskeletal and sarcomeric	3.75	1.4271E-07
maker-ptg0002151-snap-gene-13.31-mRNA-1	S100b	Cytosolic Ca2+-binding protein of the EF-hand superfamily	S100 calcium binding protein B	Signaling	8.14	1.0122E-22
maker-ptg0000491-snap-gene-23.20-mRNA-1	FGF12	Possibly regulate voltage-gated sodium channels	Fibroblast growth factor 12	Signaling	8.72	5.8498E-17
maker-ptg0008381-snap-gene-3.218-mRNA-1	NDRG3	Predicted to be involved in signal transduction	N-Myc downstream-regulated gene 3 protein	Signaling	11.02	7.4446E-08
maker-ptg0015631-augustus-gene-5.35-mRNA-1	SGK1	Serine/threonine-protein kinase	Serine/threonine-protein kinase Sgk1	Signaling	7.79	6.6327E-38
maker-ptg0010881-snap-gene-0.7-mRNA-1	SIX2a	Target ARE promoter elements in sodium/potassium adenosine triphosphatases	SIX homeobox 2	Transcription factor	3.05	1.221E-27
maker-ptg0007831-snap-gene-6.78-mRNA-1	HEY1	Developing cardiac conduction pathway	Hes-related family bHLH transcription factor with YRPW motif 1	Transcription factor	6.02	1.5325E-13
maker-ptg0017401-augustus-gene-1.112-mRNA-1	KLF5	Rebalance potassium channels	Krüppel-like factor 5	Transcription factor	8.39	5.0491E-06
maker-ptg0000081-snap-gene-10.43-mRNA-1	MEF2a	Transcriptional activator for numerous muscle-specific genes	Myocyte-specific enhancer factor 2A	Transcription factor	3.85	3.7818E-50
maker-ptg0012701-snap-gene-47.16-mRNA-1	MEF2b	Transcriptional activator for numerous muscle-specific genes	Myocyte-specific enhancer factor 2B	Transcription factor	6.92	8.4583E-68
maker-ptg0009701-augustus-gene-2.127-mRNA-1	ATP1a1	Sodium/potassium-ATPase $\alpha$ -subunit	Sodium/potassium-transporting ATPase subunit alpha-1	Transmembrane ion transport	10.55	2.1894E-05
snap_masked-ptg0011561-processed-gene-0.19-mRNA-1	ATP1a2a	Sodium/potassium-ATPase $\alpha$ -subunit	Sodium/potassium-transporting ATPase subunit alpha-2	Transmembrane ion transport	3.07	2.6317E-12
maker-ptg0010471-snap-gene-1.63-mRNA-1	ATP1b1a	Sodium/potassium-ATPase $\beta$ -subunit	ATPase sodium/potassium transporting beta 1a	Transmembrane ion transport	6.59	3.6325E-59
maker-ptg0005091-snap-gene-9.39-mRNA-1	ATP1b1b	Sodium/potassium-ATPase $\beta$ -subunit	ATPase sodium/potassium transporting beta 1b	Transmembrane ion transport	4.51	2.0647E-06
maker-ptg0000281-snap-gene-81.10-mRNA-1	KCNA7a_1	Kv channel	Potassium voltage-gated channel subfamily A member 7a	Transmembrane ion transport	4.60	2.5847E-11
maker-ptg0000281-snap-gene-81.8-mRNA-1	KCNA7a_2	Kv channel	Potassium voltage-gated channel subfamily A member 7a	Transmembrane ion transport	8.27	3.5553E-12
maker-ptg0014271-snap-gene-13.20-mRNA-1	KCNIP3	Kv channel	Calsenilin	Transmembrane ion transport	5.11	0.00099357

(continued)

Table 1 (continued)

ID	Blast gene	Highlights of predicted function	Gene description	Category	Average $\log_2FC$	Average P-value
maker-ptg0006971-snap-gene-6.109-mRNA-1	KCNQ5	Kv channel	Potassium voltage-gated channel subfamily Q member 5	Transmembrane ion transport	5.94	0.00093894
maker-ptg0002651-est_gff_est2genome-gene-6.33-mRNA-1	KCNJ2	Kir channel	Inward rectifier potassium channel 2	Transmembrane ion transport	5.53	1.1222E-20
maker-ptg0008301-augustus-gene-5.123-mRNA-1	KCNJ9	Kir channel	G protein-activated inward rectifier potassium channel 3	Transmembrane ion transport	5.77	2.6324E-10
snap_masked-ptg0011181-processed-gene-0.13-mRNA-1	KCNK2	K2p channel	Potassium channel subfamily K member 2	Transmembrane ion transport	6.15	9.238E-14
maker-ptg0002531-augustus-gene-20.10-mRNA-1	SCN1ba	Nav channel	Sodium channel subunit beta-1	Transmembrane ion transport	3.84	1.2983E-07
maker-ptg0011881-snap-gene-6.4-mRNA-1	SCN4aa	Nav channel	Sodium channel protein type 4 subunit alpha A	Transmembrane ion transport	10.98	1.2737E-11
maker-ptg0022391-snap-gene-5.5-mRNA-1	SCN4b	Nav channel	Sodium voltage-gated channel beta subunit 4	Transmembrane ion transport	5.34	8.1806E-47
maker-ptg0001481-snap-gene-9.4-mRNA-1	SLC24a2	Calcium, potassium:sodium antiporter	Solute carrier family 24 member 2	Transmembrane ion transport	9.06	1.1057E-37

EOD, e.g. membrane, Golgi membrane and apparatus, calcium ion binding, and ATP binding.

### Allele-Specific Expression in F1 Hybrids

Two cohorts of F1 hybrids with 1 short-duration EOD (*com* × *tsh*) and 1 medium-duration EOD (*com* × *rhy*) were analyzed in our study. In total, we identified fixed single nucleotide polymorphisms (SNPs; homozygous in parental species) in 177 genes differentially expressed in EO and in 52 differentially expressed in SM in the hybrid *com* × *rhy*. For the hybrid *com* × *tsh*, the respective SNP numbers were 77 in genes differentially expressed in the EO and 36 in genes differentially expressed in the SM (Fig. 5a). For each of these genes, we calculated the allelic read proportion of the allele stemming from the parental species *com* (as identified by the fixed SNPs), averaged over the specimens of the respective hybrid cohort. In general, most genes exhibit an equal expression of both parental alleles, with more genes having a *com* proportion near 0.5 (Fig. 5a). Among the genes with differentially expressed alleles, alleles stemming from *com* had an overall tendency toward higher expression, compared to the alleles from *rhy* or *tsh*, in both EO and SM from 2 hybrid cohorts (Fig. 5a).

In order to understand the allelic expression imbalance (AEI), we counted the number of genes with more than 0.6 proportion of 1 parental allele proportion for all individuals in each analyzed hybrid set (Chang et al. 2002). In total, we identified 17 and 7 genes with AEI in EO and SM of the hybrid *com* × *rhy*, respectively; 2 and 1 such genes were identified in EO and SM of the hybrid *com* × *tsh*, respectively (supplementary table S7, Supplementary Material online). In all the genes with AEI, the allele from *com* showed a higher expression proportion, except for the gene *KCNJ2* in the hybrid *com* × *rhy* where allele expression was biased in the opposite direction (average proportion of *com* allele was 0.16; Fig. 5b). We inferred amino acid sequences from the transcript sequences of the *KCNJ2* gene from *com*, *tsh*, and *rhy*. The inferred protein sequences between *com* and *tsh* were identical, but *rhy* showed 2 amino acid substitutions at sites 60 (corresponding to the fixed SNP we identified in hybrids) and 198 (supplementary table S8, Supplementary Material online). The amino acid substitution at site 60 was considered benign in the Polyphen2 analysis (Adzhubei et al. 2010), while the substitution at site 198 may have changed the protein function in *rhy* (inferred as probably damaging; supplementary table S9, Supplementary Material online).

We also identified AEI in the gene *SCN4aa* in the EO of *com* × *rhy* hybrids (average proportion of *com* allele was 0.66; Fig. 5b). This proportion of the *com* allele is much higher than in the hybrid *com* × *tsh*, where the *com* allele of the *SCN4aa* only had a proportion of 0.46 in the EO. In the EO of hybrid *com* × *rhy*, AEI was identified in the gene *CHRND*, which might relate to ion channel gating (Fig. 5b). The *TSPAN6b* gene, encoding for an integral component of the plasma membrane, was also identified to exhibit a significant AEI in the EO of hybrid *com* × *tsh* (average proportion of *com* allele was 0.86; Fig. 5b).

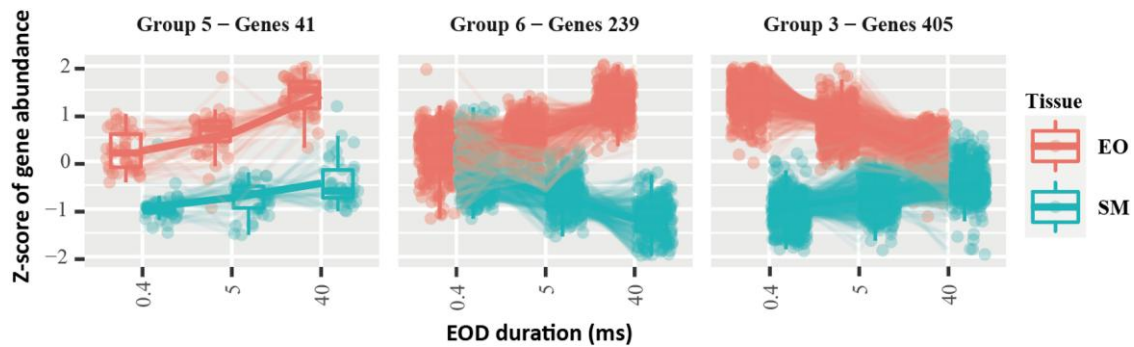


**Fig. 4.** RNA-seq data clustered by EOD duration (only for the 3 purebred species).

**Table 2** Genes with expression correlated to EOD duration and their description

Group	Gene ID in annotation	Gene	Highlights of predicted function	Gene description	Category
3	maker-ptg0003611-augustus-gene-0.2-mRNA-1	<i>ACTR3b</i>	F-actin dynamics/polymerization	ARP3 actin-related protein 3 homolog B	Cytoskeletal and sarcomeric
3	maker-ptg000509l-snap-gene-4.4-mRNA-1	<i>NHS</i>	Regulator of actin remodeling	Nance–Horan syndrome protein	Cytoskeletal and sarcomeric
3	maker-ptg001966l-augustus-gene-18.42-mRNA-1	<i>KCNK6</i>	Outward rectification in a physiological potassium gradient and mild inward rectification in symmetrical potassium conditions	Potassium channel subfamily K member 6	Transmembrane ion transport
3	maker-ptg000697l-snap-gene-6.109-mRNA-1	<i>KCNQ5</i>	Voltage-gated potassium channel	Potassium voltage-gated channel subfamily Q member 5	Transmembrane ion transport
5	maker-ptg000265l-est_gff_est2genome-gene-6.33-mRNA-1	<i>KCNJ2</i>	Inwardly rectifying potassium channel	Inward rectifier potassium channel 2	Transmembrane transport
5	maker-ptg001740l-augustus-gene-1.112-mRNA-1	<i>KLF5</i>	Transcription factor, which might regulate potassium channel genes	Krüppel-like factor 5	Transcription factor

## Discussion

### Convergent Gene Expression in Different Electric Fish Lineages

The myogenic EO has convergently evolved 6 times in fishes. Even though the EOs show great differences in electrocyte morphology among independently evolved electric fish lineages, particular genes exhibit similar transcriptional expression patterns in the EO, relative to SM (Gallant et al. 2014).

Several EO-specific candidate genes that we identified in *Campylomormyrus* were also overexpressed in the EO of other electric fish lineages, possibly indicating convergent expression pattern evolution in electric fish. This is

particularly apparent in genes related to sodium and potassium currents. For instance, the  $Na_v$  channel gene *SCN4aa*, considered to be very important in regulating the sodium current to electrocytes, was previously found overexpressed in the EO of different electric fish lineages, i.e. Siluriformes, Gymnotiformes, and Mormyridae other than *Campylomormyrus* (Wang and Yang 2021). The *FGF13a* that regulates this channel was consistently overexpressed in those electric fish species as well (Gallant et al. 2014). Interestingly, we identified another upregulated ortholog (*FGF12*) in the EO, which may have a similar function. In addition, multiple isoforms of sodium/potassium-ATPase  $\alpha$ - and  $\beta$ -subunits and several transcription factors (*SIX2a*, *HEY1*) were found to be



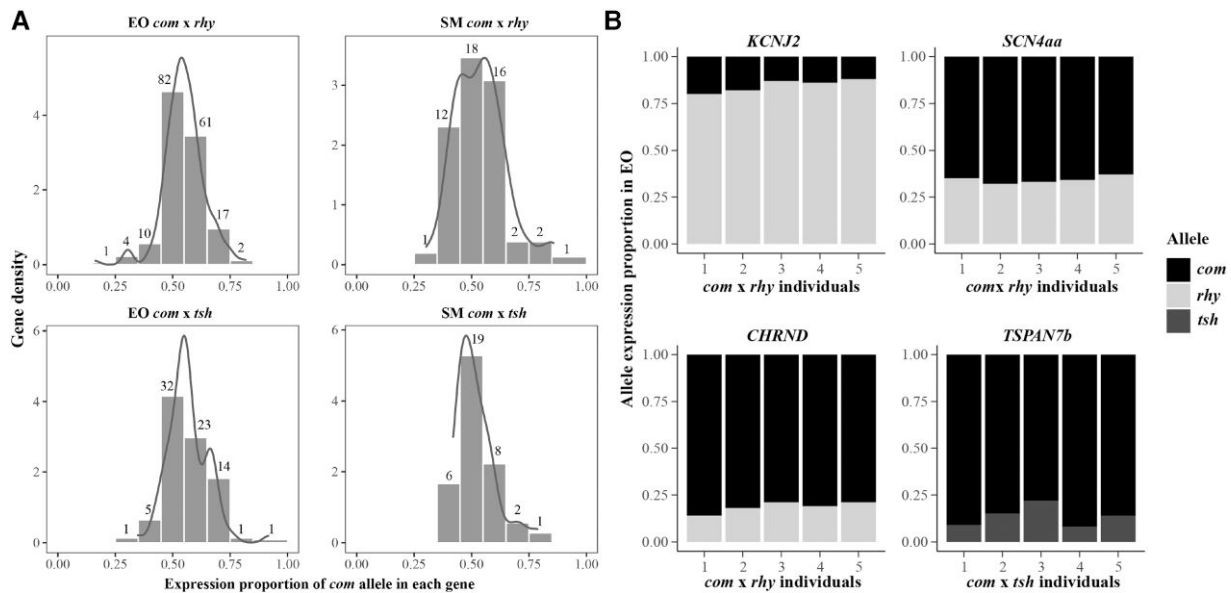


**Fig. 5.** Allele-specific expression in EO and SM among 2 hybrid cohorts *C. compressirostris* (*com*) × *C. rhynchophorus* (*rhy*) and *C. compressirostris* (*com*) × *C. tshokwe* (*tsh*). a) Gene density (y-axis) from two different tissues in each hybrids. The x-axis shows the expression proportion of the allele stemming from one parental species (*com*). Numbers above the bars represent the number of genes in the respective proportion ranges. b) Proportion of two alleles from parental species in four genes related to ion transport and membrane (*KCNJ2*, *SCN4AA*, *CHRND* and *TSPAN7b*) in the EO. The x-axis represents the different individual samples of the corresponding hybrid cohort.

convergently upregulated in the EO among these electric fish lineages (Gallant et al. 2014), a pattern confirmed for *Campylomormyrus* in our study.

Overexpression of another transcription factor (*MEF2a*) and of the calcium binding gene *S100b* is characteristic for mormyrid EOs, i.e. *Paramormyrops*, *Brienomyrus* (Gallant et al. 2012, 2017), and *Campylomormyrus* (this study). We recently found *KCNA7a* to be tandemly duplicated in *Campylomormyrus* (Cheng et al. 2023) and *Paramormyrops* (by reanalysis of the genome provided in Gallant et al. 2017). This tandem duplication might be exclusive to mormyrid fishes, as we did not find it in available genomes neither of other electric fishes nor in *Scleropages* (a nonelectric fish closely related to mormyrids; data not shown). In our study, both gene copies *KCNA7a\_1* and *KCNA7a\_2* were consistently upregulated in the EO (*KCNA7a\_2* showed even higher expression than *KCNA7a\_1*). *KCNA7a* was inferred to be under positive selection in the transmembrane helix 3 and 4 linkers and is considered to relate to the differences in EOD duration among *Brienomyrus* and *Gymnarchus* (Swapna et al. 2018).

The *NDRG3* gene (N-Myc Downstream-Regulated Gene 3) exhibited a remarkable overexpression in the EO of *Campylomormyrus*. Interestingly, the phosphopeptides encoded by an ortholog (*NDRG4*) were highly enriched in the EO of the strongly discharging gymnotiform electric eel (*Electrophorus electricus*; Traeger et al. 2017), indicating high expression level of this gene. In addition, *NDRG4* has been identified in zebrafish as a novel neuronal factor essential for sodium channel clustering at the nodes of Ranvier, the only places where action potentials are regenerated (Fontenas et al. 2016). The function of *NDRG3* in the nervous system has rarely been investigated. The

*NDRG3* protein can interact with extracellular signal-regulated kinases (ERK1/2; Lee et al. 2015), which regulate  $K_{v4.2}$  in the dendrites of hippocampal CA1 pyramidal neurons (Schrader et al. 2006; Gupte et al. 2016) as well as the  $Na_v1.7$  channel (Stambouljian et al. 2010). In porcine as well as human lens, ERK1/2 is activated by the TRPV1 ion channel (Mandal et al. 2019), which was also overexpressed in EOs in *Campylomormyrus* (supplementary table S1, Supplementary Material online).

### Gene Expression Specificity in *Campylomormyrus*

The EO in mormyrids is derived from myogenic tissue, which transitions from a motoric/sarcomeric organization of muscle fibers to a continuous tube of electrocytes parallel to the spinal cord (Denizot et al. 1982). This transition process during the ontogeny of the EO involves cell size, morphology, and physiology and is still only partially understood. Some genes encoding for sarcomeric proteins, e.g. troponin I isoforms, myosin heavy chain, and tropomyosin, are overexpressed in the EO of the mormyrid *Brienomyrus brachyistius* (Gallant et al. 2012), providing a preliminary insight into the developmental transition from SM to EO. In the EO of *Campylomormyrus*, however, we rarely found those genes upregulated. Instead, the upregulated actin-related genes in *Campylomormyrus* were more related to F-actin dynamics and included several unconventional myosins (Table 1; supplementary table S1, Supplementary Material online). The 4 paralogous transcription factors *MEF2a* to *MEF2d* are responsible for the transcriptional activation of muscle-specific genes in the early specification of SM (Black and Olson 1998). Whereas *MEF2a* was overexpressed in the EOs of both *Brienomyrus* (Gallant et al. 2012) and *Campylomormyrus*,

a further paralog *MEF2b* was overexpressed only in *Campylomormyrus* (our study). The difference in expression of F-actin-related/sarcomeric proteins and *MEF2* transcription factors between 2 mormyrids genera suggests that the developmental transition in the EO might be different or, in other words, that the organization of the F-actin system in electrocytes may vary across mormyrids. It has to be analyzed further whether these differences in the organization of the F-actin cytoskeleton concern the sarcomeric structure, the stalks of electrocytes, or both.

In addition, 2 paralogs of inwardly rectifying potassium channel ( $K_{ir}$ ) genes, *KCNJ2* and *KCNJ9*, were overexpressed in EOs of *Campylomormyrus*, along with *KCNQ5* and *KCNK2*. The mechanisms regulating potassium channels' expression in electric fish are still unknown. We identified 1 transcription factor, *KLF5*, that showed a high overexpression in EOs. In *Drosophila*, Krüppel is involved in the regulation of potassium channel expression. In case of a loss of *Shal* (*KCND*) potassium channel in *Drosophila*, Krüppel expression is induced and upregulates expression of *Shaker* (*KCNA*) and *slowpoke* ( $K_{ca}$ ) potassium channels (Parrish et al. 2014). Remarkably, *Shal* (*KCND*) potassium channel is also not expressed in our studied *Campylomormyrus* species/hybrids. We thus suppose that the EO differs from SM by the expression of a unique set of potassium channels that may contribute to the shape of the EO's action potential and thus the shape of the EOD signal. Moreover, we propose the *KLF5* gene to represent a transcription factor that drives the expression of regulating potassium channels in EO.

Our study has further revealed that different paralogs from the solute carrier family are active in EOs. Solute carriers form a group of membrane transport proteins located in various cellular membrane systems, which transport diverse substrates including amino acids, oligopeptides, inorganic cations, and anions (He et al. 2009). We have found several genes of this gene family overexpressed in the EO that transport inorganic cations and anions, e.g. sodium, calcium, and chloride. Especially the gene *SLC24a2* was highly overexpressed in *Campylomormyrus* EOs. This is a calcium/cation antiporter localized in the plasma membrane that mediates the extrusion of 1 calcium ion and 1 potassium ion in exchange for 4 sodium ions (Wang et al. 2017). Overexpression of a calcium-extruding transporter in the EO indicates that regulation of the cytosolic calcium level in electrocyte differs from that in SM. Unfortunately, we have no information yet on the distribution of the *SLC24a2* protein within the electrocytes and whether this calcium transporter is confined to a distinct region of the cell to mediate local regulation of the calcium level.

### Differential Gene Expression with Respect to EOD Duration Divergence among *Campylomormyrus* Species

*Campylomormyrus* species produce species-specific EODs; their duration varies in a 100-fold range across species. The EOD is assumed to be mediated by sodium and potassium

currents across the plasma membrane (Stoddard and Markham 2008). The depolarizing phase of an action potential is primarily produced by sodium influx. The repolarization phase is—along with a gradual decreasing sodium influx—affected by the orchestrated activities of delayed rectifier and inward rectifier potassium channels (Nass et al. 2008; Stoddard and Markham 2008). We suppose that species producing EODs of different duration may be equipped with different channel types or channel orthologs with different properties. However, certain other mechanisms, such as different cell morphology, may also contribute to the EOD duration diversification.

The PCA from RNA-seq data showed a clear association between the overall gene expression and the EOD duration pattern (Fig. 3a). Based on the preliminary PCA and LRT result, we identified several genes that might contribute to EOD duration diversification in *Campylomormyrus*, including the potassium channel genes (*KCNJ2*, *KCNK6*, and *KCNQ5*), actin-related genes (*ACTR3b*, *NHS*), and transcription factor *KLF5* (Table 2).

The gene *KCNK5* was found to be upregulated in *Paramormyrops* (producing a short EOD) compared to the species with an elongated EOD (Losilla et al. 2020). In *Campylomormyrus*, the expression of another paralog *KCNK6* was also higher in species with short EOD. Two-pore potassium channels ( $K_{2p}$ ) usually generate an outward potassium current and are also known as potassium leak channels. When silencing the *KCNK6* gene in the human heart, the action potential duration is prolonged (Chai et al. 2017). Another voltage-gated potassium channel gene *KCNQ5* was decreasingly expressed in elongated EOD *Campylomormyrus* species. It forms M-type potassium current, a slowly activating and deactivating potassium conductance that works in determining the subthreshold electrical excitability of neurons (Hibino et al. 2010). The lower expression of both potassium channel genes in elongated EOD species will probably decrease the outward potassium current and consequently prolongate EOD repolarization.

The gene *KCNJ2* was increasingly expressed in elongated EOD species. It encodes for an  $K_{ir}$ , with the greater tendency to allow potassium ions to flow into a cell rather than out of a cell (Hibino et al. 2010). The inward potassium current stabilizes the resting membrane potential of the cell and modulates the cardiac repolarization processes (Hibino et al. 2010; Li et al. 2017). This inward rectifier channel-mediated potassium current is responsible for shaping the initial depolarization and final repolarization of the action potential in human cardiomyocytes (Dhamoon and Jalife 2005; Jeevaratnam et al. 2018).

Regarding allele-specific expression, the 26 genes with AEI (supplementary table S7, Supplementary Material online) in F1 hybrids were related to ion transport, plasma membrane, and myofibrils in the EO and actin in the SM (supplementary table S10, Supplementary Material online). The imbalance could be caused by *cis*-regularity differences among the parental species in the upstream transcription unit (e.g. a promoter; Landry et al. 2007). There was a tendency toward higher expression of *com*

alleles in the EOs and SMs of 2 analyzed hybrid cohorts (Fig. 5a; supplementary table S7, Supplementary Material online). However, the phenotype of the EOD waveform in each hybrid is closer to the other parental species. This points toward some genes playing key roles in regulating the EOD waveform in the hybrids. The gene *KCNJ2* showed AEI in *com* × *rhy* hybrids, which was the only gene with AEI and for which the *rhy* allele was preferentially expressed (Fig. 5b). The EOD in the adult hybrids *com* × *rhy* was of intermediate duration (4 ms), and the shape and waveform resemble the subadults' EOD in *rhy*. Both the EOD phenotype and the AEI in *KCNJ2* were hence closer to the parental species with the elongated EOD, i.e. *rhy*. The expression of *KCNJ2* in the EO among the purebred species also increased with increasing EOD duration, e.g. the expression in *rhy* is higher than in *com*. This suggests that the *KCNJ2* gene might be under *cis*-regulation, and it should be a powerful candidate gene involved in the regulation of EOD duration in *Campylomormyrus*.

In addition, the *KCNJ2* gene in the species *rhy* (very long EOD) exhibits 2 nonsynonymous substitutions, one of which predicted to cause a functionally relevant amino acid substitution (at site 198; supplementary tables S8 and S9, Supplementary Material online). Interestingly, the same substitution at site 198 is present in another species with very long EOD (*C. numenius*, EOD duration 40 ms), while it is absent in other *Campylomormyrus* species with short or medium EOD, which resemble the amino acid sequence of *com* and *tsh* (Cheri, Cheng, and Tiedemann, unpublished results). *Campylomormyrus numenius* and *rhy* are phylogenetically close (Lamanna et al. 2016), such that the shared amino acid substitution could also reflect phylogenetic affinity. Nonetheless, the found amino acid substitution with inferred functional relevance could relate to the evolution of very long EODs in *Campylomormyrus*. Then, the *KCNJ2* gene could modulate EOD duration by a combination of expression level and functional protein sequence alteration. In summary, this study identifies the *KCNJ2*, *KCNK6*, and *KCNQ5* genes, possibly in combination with other genes (e.g. *KLFS*, *ACTR3b*, and *NHS*) as strong candidates underlying EOD duration diversification in the weakly electric fish genus *Campylomormyrus*. The diverged EODs likely affect the food spectrum and are used for mate recognition. This potential dual function in disruptive natural selection and prezygotic reproductive isolation would rank the EOD as a “magic trait,” which may have promoted the ecological (probably sympatric) speciation and radiation of *Campylomormyrus* in the Congo River.

## Materials and Methods

### Animals, RNA Isolation, Library Preparation, and Sequencing

Three adult specimens of *C. tshokwe* were collected at Brazzaville/Republic of the Congo in the Congo River in 2012 and stored in RNAlater in  $-80^{\circ}\text{C}$ . Five adult

specimens from each of the other 2 species (*C. compressirostris*, *C. rhynchophorus*) and 2 hybrids (*C. compressirostris* ♂ × *C. rhynchophorus* ♀, *C. compressirostris* ♂ × *C. tshokwe* ♀) were artificially bred and raised at the University of Potsdam. All specimens except for *C. tshokwe* were anesthetized by a lethal dose of clove oil and dissected on cold 99% ethanol. EO and SM tissues from each specimen were flash frozen in liquid nitrogen and further preserved in  $-80^{\circ}\text{C}$ . In total, we collected 3 samples of both EOs and SMs from *C. tshokwe* and 5 samples of both EOs and SMs from the other 4 species/hybrid cohorts in this study.

The RNA isolation was performed in all the EO and SM samples using QIAGEN RNeasy Fibrous Tissue Mini Kit. Total RNA concentration was estimated using a NanoDrop 1000 spectrophotometer (Thermo Fisher Scientific, Germany), and RNA quality was checked with an Agilent Bioanalyzer 2100 (Agilent Technologies, United States). mRNA enrichment was performed by poly(A) capture from isolated RNA using NEXTflex Poly(A) Beads. Strand-specific transcriptomic libraries were built using NEXTflex Rapid Directional RNA-Seq Kit (Bioo Scientific, United States) based on the manufacturer's instructions.

Libraries were sequenced as 150 bp paired-end reads by Illumina HiSeq 4000 sequencing system at a commercial company (Novogene). Raw reads have been deposited in the National Center for Biotechnology Information (NCBI) Gene Expression Omnibus (accession number GSE240783). We trimmed the adapter sequences and low-quality reads using a 4 bp sliding window with a mean quality threshold of 25 and a minimum read length of 36 bp by Trimmomatic v0.39 (Bolger et al. 2014). Read quality, before and after read filtering, was measured by FastQC v0.11.9 (Andrew 2010).

### Differential Gene Expression Analysis

The quality-filtered reads from EOs and SMs were mapped to the *C. compressirostris* genome (Cheng et al. 2023) using RSEM (Li and Dewey 2011) for gene-level quantification estimation. The estimated counts were imported into R/Bioconductor with the tximport package (Soneson et al. 2015), which produced count matrices from gene-level quantification by taking the effective gene length into account (Paraskevopoulou et al. 2020). Low-count ( $\leq 10$ ) and low-frequency (not present in at least 2 replicates) genes were removed. We performed a PCA from filtered and log-transformed counts. One SM sample from *C. compressirostris* was removed from this study, as its overall gene expression showed a deviant unusual pattern in the PCA.

We forwarded the normalized count matrices to DESeq2 (Love et al. 2014) to infer expression differences among EO and SM in each species/hybrid cohort, respectively. We used a false discovery rate threshold of 0.05 to correct for multiple testing. The DEGs were identified with  $|\log_2\text{FC}| > 1$  and  $P < 0.05$ . In order to detect the EO-specific gene expression pattern, we used Venn diagrams (Chen and Boutros 2011) to visualize the shared

DEGs (up- and downregulated separately) among 3 purebred species and 2 hybrid cohorts.

The shared DEGs were annotated against the NCBI *nr* database by blastx with an *e*-value cutoff of  $1E^{-10}$ . In addition, the up- and downregulated DEGs in the EO were used to perform a GO enrichment analysis (Dennis et al. 2003).

### RNA-seq Data Clustering by EOD Duration

The PCA plotting from log-transformed count matrices showed a clear pattern by the length of EOD (Fig. 3a). To identify genes with an expression pattern associated to EOD duration, we used DESeq2 to perform a LRT (Love et al. 2015; LRT in the DESeq2 package). This test compares how well a gene's count data fit a "full model" compared to a "reduced model" (Bendjilali et al. 2017). Our full model was an equation: full = ~duration × tissue. The duration is the length of the EOD in each purebred species, and tissue is the type of sample (EO or SM). The reduced model excluded the interaction between duration and tissue: reduced = ~duration + tissue. Genes with  $P_{adj} < 0.05$  were considered to fit the "full model." We used the degPatterns function from the "DEGreport" package to cluster different groups with particular expression pattern using those significant genes across samples (Pantano 2019), with time = "duration" and col = "tissue."

The generated groups of different gene expression pattern across EOD duration were analyzed to identify genes with an expression pattern association with EOD duration. We hence focused on those groups fulfilling the following 2 criteria: (i) the gene expression level in EO is higher than SM in all F0 species, and (ii) the gene expression level in EO across EOD duration showed a consistent increasing or decreasing pattern.

The identified genes with increased and decreased expression relative to EOD duration were blasted against *nr* database using an *e*-value cutoff of  $1E^{-10}$ . In addition, a GO term analysis was also performed for these genes.

### Allelic-Specific Expression Analysis

The F1 hybrid contains 2 sets of subgenome from 2 parental species. Examination of allele-specific expression can be applied to detect the allelic imbalance in transcription in heterozygous F1 hybrids. We only focused on transcripts of genes with biallelic SNPs fixed among the respective F0 parental species (hence, heterozygous only in F1 hybrids and homozygous in parental species).

We mapped the trimmed and filtered RNA-seq from 5 species/hybrids (in EOs and SMs, respectively) to the *C. compressirostris* genome using STAR v2.7.7 (Dobin and Gingeras 2015). The generated bam files were sorted according to the coordinates by SAMtools v1.15 (Danecek et al. 2021). Variant calling was performed by BCftools v1.9 (Danecek et al. 2021) in EOs and SMs, respectively, using the command "bcftools mpileup -f REFERENCE LIST\_OF\_BAM -Ou | bcftools call -mv -Ob -o BCFFILE," where the REFERENCE, LIST\_OF\_BAM, and

BCFFILE were the CDS sequence name of the *C. compressirostris* genome, the list of bam files, and the output bcf file name, respectively.

After the variant calling, we performed the following steps to identify the fixed parental biallelic SNPs for each hybrid set. Firstly, we excluded the uncalled variants and only preserved biallelic SNPs using the command "bcftools view --exclude-uncalled -m2 -M2 BCFFILE > CALLING\_AD," where the CALLING\_AD was the allelic depth for the final biallelic SNPs. Secondly, we discarded SNPs where the variant calling score at QUAL field was lower than 70, and allelic depth was lower than 10 in both alleles. Finally, we obtained high-quality SNPs, at which both parental species were homozygous and fixed for a different allele.

For each hybrid, we calculated the expression proportion of the allele from *C. compressirostris* in EO and SM, respectively. We calculated the average proportion and its 95% confidence limits across biological replicates (and over SNPs in case of more than 1 SNP per locus; Fig. 5; supplementary table S7, Supplementary Material online). Genes with *C. compressirostris* allele proportions  $< 0.4$  or  $> 0.6$  in the transcriptomes were considered exhibiting an imbalanced expression. We further applied GO analysis on the genes with AEI for EO and SM, respectively.

### Supplementary Material

Supplementary material is available at *Molecular Biology and Evolution* online.

### Acknowledgments

We thank Dr. Linh Nguyen for fish breeding and raising. All figures were edited with Biorender.com.

### Author Contributions

R.T. conceived and supervised this study and provided financial and logistical support. F.C. performed lab work, analysis, and manuscript writing with the input from R.T., A.B.D., O.B., F.K., and S.A.-S.

### Funding

This project is funded by the University of Potsdam.

### Conflict of Interest

None declared.

### Data Availability

Sequence data have been deposited at NCBI Gene Expression Omnibus under accession number GSE240783.

### References

Adzhubei IA, Schmidt S, Peshkin L, Ramensky VE, Gerasimova A, Bork P, Kondrashov AS, Sunyaev SR. A method and server for

- predicting damaging missense mutations. *Nat Methods*. 2010;7(4):248–249. <https://doi.org/10.1038/nmeth0410-248>.
- Andrew S. FastQC: a quality control tool for high throughput sequence data. *Babraham Bioinformatics*. 2010. [www.bioinformatics.babraham.ac.uk/projects/fastqc/](http://www.bioinformatics.babraham.ac.uk/projects/fastqc/).
- Bass A. Electric organs revisited: evolution of a vertebrate communication and orientation organ. In: Bullock TH, Heiligenberg W, editors. *Electroreception*. New York: Wiley p; 1986. p. 13–70.
- Bendjilali N, MacLeon S, Kalra G, Willis SD, Hossian AKMN, Avery E, Wojtowicz O, Hickman MJ. Time-course analysis of gene expression during the *Saccharomyces cerevisiae* hypoxic response. *G3 (Bethesda)*. 2017;7(1):221–231. <https://doi.org/10.1534/g3.116.034991>.
- Black BL, Olson EN. Transcriptional control of muscle development by myocyte enhancer factor-2 (MEF2) proteins. *Annu Rev Cell Dev Biol*. 1998;14(1):167–196. <https://doi.org/10.1146/annurev.cellbio.14.1.167>.
- Bolger AM, Lohse M, Usadel B. Trimmomatic: a flexible trimmer for Illumina sequence data. *Bioinform*. 2014;30(15):2114–2120. <https://doi.org/10.1093/bioinformatics/btu170>.
- Chai S, Wan X, Nassal DM, Liu H, Moravec CS, Ramirez-Navarro A, Deschênes I. Contribution of two-pore K<sup>+</sup> channels to cardiac ventricular action potential revealed using human iPSC-derived cardiomyocytes. *Am J Physiol Heart Circ Physiol*. 2017;312(6):H1144–H1153. <https://doi.org/10.1152/ajpheart.00107.2017>.
- Chang HW, Lee SM, Goodman SN, Singer G, Cho SKR, Sokoll LJ, Montz FJ, Roden R, Zhang Z, Chan DW, et al. Assessment of plasma DNA levels, allelic imbalance, and CA 125 as diagnostic tests for cancer. *J Nat Cancer Inst*. 2002;94(22):1697–1703. <https://doi.org/10.1093/jnci/94.22.1697>.
- Chen H, Boutros PC. VennDiagram: a package for the generation of highly-customizable Venn and Euler diagrams in R. *BMC Bioinform*. 2011;12(1):1–7. <https://doi.org/10.1186/1471-2105-12-35>.
- Cheng F, Dennis AB, Osuoha J, Canitz J, Kirschbaum F, Tiedemann R. A new genome of an African weakly electric fish (*Campylomormyrus compressirostris*, Mormyridae) indicates rapid gene family evolution in Osteoglossomorpha. *BMC Genom*. 2023;24(1):129. <https://doi.org/10.1186/s12864-023-09196-6>.
- Danecek P, Bonfield JK, Liddle J, Marshall J, Ohan V, Pollard MO, Whitwham A, Keane T, McCarthy SA, Davies RM. Twelve years of SAMtools and BCFtools. *Gigascience* 2021;10(2):1–4. <https://doi.org/10.1093/gigascience/giab008>.
- Darwin C. *On the origin of species*. London: Murray; 1859.
- Denizot JP, Kirschbaum F, Westby GWM, Tsuji S. On the development of the adult electric organ in the mormyrid fish *Pollimyrus isidori* (with special focus on the innervation). *J Neurocytol*. 1982;11(6):913–934. <https://doi.org/10.1007/BF01148308>.
- Dennis G, Sherman BT, Hosack DA, Yang J, Gao W, Lane HC, Lempicki RA. DAVID: database for annotation, visualization, and integrated discovery. *Genome Biol*. 2003;4(9):1–11. <https://doi.org/10.1186/gb-2003-4-9-r60>.
- Dharmoon AS, Jalife J. The inward rectifier current (I<sub>K1</sub>) controls cardiac excitability and is involved in arrhythmogenesis. *Heart Rhythm* 2005;2(3):316–324. <https://doi.org/10.1016/j.hrthm.2004.11.012>.
- Dobin A, Gingeras TR. Mapping RNA-seq reads with STAR. *Curr Protoc Bioinformatics*. 2015;51(1):11–14. <https://doi.org/10.1002/0471250953.bi1114s51>.
- Feulner PGD, Plath M, Engelmann J, Kirschbaum F, Tiedemann R. Electrifying love: electric fish use species-specific discharge for mate recognition. *Biol Lett*. 2009a;5(2):225–228. <https://doi.org/10.1098/rsbl.2008.0566>.
- Feulner PGD, Plath M, Engelmann J, Kirschbaum F, Tiedemann R. Magic trait electric organ discharge (EOD): dual function of electric signals promotes speciation in African weakly electric fish. *Commun Integr Biol*. 2009b;2(4):329–331. <https://doi.org/10.4161/cib.2.4.8386>.
- Fontenas L, De Santis F, Di Donato V, Degerny C, Chambraud B, Del Bene F, Tawk M. Neuronal NdrG4 is essential for nodes of ranvier organization in zebrafish. *PLoS Genet*. 2016;12(11):1–24. <https://doi.org/10.1371/journal.pgen.1006459>.
- Gallant JR, Arnegard ME, Sullivan JP, Carlson BA, Hopkins CD. Signal variation and its morphological correlates in *Paramormyrops kingsleyae* provide insight into the evolution of electrogenic signal diversity in mormyrid electric fish. *J Comp Physiol A*. 2011;197(8):799–817. <https://doi.org/10.1007/s00359-011-0643-8>.
- Gallant JR, Hopkins CD, Deitcher DL. Differential expression of genes and proteins between electric organ and skeletal muscle in the mormyrid electric fish *Brienomyrus brachyistius*. *J Exp Biol*. 2012;215(14):2479–2494. <https://doi.org/10.1242/jeb.063222>.
- Gallant JR, Losilla M, Tomlinson C, Warren WC. The genome and adult somatic transcriptome of the mormyrid electric fish *Paramormyrops kingsleyae*. *Genome Biol Evol*. 2017;9(12):3525–3530. <https://doi.org/10.1093/gbe/evx265>.
- Gallant JR, Traeger LL, Volkening JD, Moffett H, Chen PH, Novina CD, Phillips GN, Anand R, Wells GB, Pinch M, et al. Genomic basis for the convergent evolution of electric organs. *Science* 2014;344(6191):1522–1525. <https://doi.org/10.1126/science.1254432>.
- Glasauer SMK, Neuhaus SCF. Whole-genome duplication in teleost fishes and its evolutionary consequences. *Mol Genet Genom*. 2014;289(6):1045–1060. <https://doi.org/10.1007/s00438-014-0889-2>.
- Gupte RP, Kadunganattil S, Shepherd AJ, Merrill R, Planer W, Bruchas MR, Strack S, Mohapatra DP. Convergent phosphomodulation of the major neuronal dendritic potassium channel Kv4. 2 by pituitary adenylate cyclase-activating polypeptide. *Neuropharmacology* 2016;101:291–308. <https://doi.org/10.1016/j.neuropharm.2015.10.006>.
- He L, Vasilou K, Nebert DW. Analysis and update of the human solute carrier (SLC) gene superfamily. *Hum Genomics* 2009;3(2):195–206. <https://doi.org/10.1186/1479-7364-3-2-195>.
- Hibino H, Inanobe A, Furutani K, Murakami S, Findlay I, Kurachi Y. Inwardly rectifying potassium channels: their structure, function, and physiological roles. *Physiol Rev*. 2010;90(1):291–366. <https://doi.org/10.1152/physrev.00021.2009>.
- Jeevaratnam K, Chadda KR, Huang CLH, Camm AJ. Cardiac potassium channels: physiological insights for targeted therapy. *J Cardiovasc Pharmacol Ther*. 2018;23(2):119–129. <https://doi.org/10.1177/1074248417729880>.
- Kim JA, Jonsson CB, Calderone T, Unguez GA. Transcription of MyoD and myogenin in the non-contractile electrogenic cells of the weakly electric fish, *Sternopygus macrurus*. *Dev Genes Evol*. 2004;214(8):380–392. <https://doi.org/10.1007/s00427-004-0421-5>.
- Kirschbaum F, Formicki K. Structure and function of electric organs. In: Kirschbaum F, Formicki K, editors. *The histology of fishes*. Boca Raton: CRC Press; 2020. p. 75–87.
- Kirschbaum F, Nguyen L, Baumgartner S, Chi HWL, Wolfart R, Elarbani K, Eppenstein H, Kornienko Y, Guido-Böhm L, Mamonekene V, et al. Intragenus (*Campylomormyrus*) and intergenus hybrids in mormyrid fish: physiological and histological investigations of the electric organ ontogeny. *J Physiol Paris*. 2016;110(3):281–301. <https://doi.org/10.1016/j.jphysparis.2017.01.003>.
- Kornienko Y, Tiedemann R, Vater M, Kirschbaum F. Ontogeny of the electric organ discharge and of the papillae of the electrocytes in the weakly electric fish *Campylomormyrus rhynchophorus* (Teleostei: Mormyridae). *J Comp Neurol*. 2021;529(5):1052–1065. <https://doi.org/10.1002/cne.25003>.
- Kuang Q, Purhonen P, Hebert H. Structure of potassium channels. *Cell Mol Life Sci*. 2015;72(19):3677–3693. <https://doi.org/10.1007/s00018-015-1948-5>.
- Lamanna F, Kirschbaum F, Ernst ARR, Feulner PGD, Mamonekene V, Paul C, Tiedemann R. Species delimitation and phylogenetic

- relationships in a genus of African weakly-electric fishes (Osteoglossiformes, Mormyridae, *Campylomormyrus*). *Mol Phylogenet Evol.* 2016;**101**:8–18. <https://doi.org/10.1016/j.ympev.2016.04.035>.
- Lamanna F, Kirschbaum F, Tiedemann R. De novo assembly and characterization of the skeletal muscle and electric organ transcriptomes of the African weakly electric fish *Campylomormyrus compressirostris* (Mormyridae, Teleostei). *Mol Ecol Resour.* 2014;**14**(6):1222–1230. <https://doi.org/10.1111/1755-0998.12260>.
- Lamanna F, Kirschbaum F, Waurick I, Dieterich C, Tiedemann R. Cross-tissue and cross-species analysis of gene expression in skeletal muscle and electric organ of African weakly-electric fish (Teleostei; Mormyridae). *BMC Genom.* 2015;**16**(1):1–17. <https://doi.org/10.1186/s12864-015-1858-9>.
- Landry CR, Hartl DL, Ranz JM. Genome clashes in hybrids: insights from gene expression. *Heredity (Edinb).* 2007;**99**(5):483–493. <https://doi.org/10.1038/sj.hdy.6801045>.
- LaPotin S, Swartz ME, Luecke DM, Constantinou SJ, Gallant JR, Eberhart JK, Zakon HH. Divergent cis-regulatory evolution underlies the convergent loss of sodium channel expression in electric fish. *Sci Adv.* 2022;**8**(22):eabm2970. <https://doi.org/10.1126/sciadv.abm2970>.
- Lee DC, Sohn HA, Park ZY, Oh S, Kang YK, Lee KM, Kang M, Jang YJ, Yang SJ, Hong YK, et al. A lactate-induced response to hypoxia. *Cell* 2015;**161**(3):595–609. <https://doi.org/10.1016/j.cell.2015.03.011>.
- Li B, Dewey CN. RSEM: accurate transcript quantification from RNA-Seq data with or without a reference genome. *BMC Bioinform.* 2011;**12**(1):1–16. <https://doi.org/10.1186/1471-2105-12-323>.
- Li M, Kanda Y, Ashihara T, Sasano T, Nakai Y, Kodama M, Hayashi E, Sekino Y, Furukawa T, Kurokawa J. Overexpression of *KCNJ2* in induced pluripotent stem cell-derived cardiomyocytes for the assessment of QT-prolonging drugs. *J Pharmacol Sci.* 2017;**134**(2):75–85. <https://doi.org/10.1016/j.jphs.2017.05.004>.
- Losilla M, Luecke DM, Gallant JR. The transcriptional correlates of divergent electric organ discharges in *Paramormyrops* electric fish. *BMC Evol Biol.* 2020;**20**(1):1–19. <https://doi.org/10.1186/s12862-019-1572-3>.
- Love MI, Anders S, Kim V, Huber W. RNA-Seq workflow: gene-level exploratory analysis and differential expression. *F1000Res* 2015;**4**:1070. <https://doi.org/10.12688/f1000research.7035.1>.
- Love MI, Huber W, Anders S. Moderated estimation of fold change and dispersion for RNA-seq data with DESeq2. *Genome Biol.* 2014;**15**(12):1–21. <https://doi.org/10.1186/s13059-014-0550-8>.
- Mandal A, Shahidullah M, Delamere NA. TRPV1-dependent ERK1/2 activation in porcine lens epithelium Amritlal. *Exp Eye Res.* 2019;**172**:128–136. <https://doi.org/10.1016/j.exer.2018.04.006>.
- Mehaffey WH, Fernandez FR, Rashid AJ, Dunn RJ, Turner RW. Distribution and function of potassium channels in the electrosensory lateral line lobe of weakly electric apteronotid fish. *J Comp Physiol A Neuroethol Sens Neural Behav Physiol.* 2006;**192**(6):637–648. <https://doi.org/10.1007/s00359-006-0103-z>.
- Nagel R, Kirschbaum F, Tiedemann R. Electric organ discharge diversification in mormyrid weakly electric fish is associated with differential expression of voltage-gated ion channel genes. *J Comp Physiol A Neuroethol Sens Neural Behav Physiol.* 2017;**203**(3):183–195. <https://doi.org/10.1007/s00359-017-1151-2>.
- Nass RD, Aiba T, Tomaselli GF, Akar FG. Mechanisms of disease: ion channel remodeling in the failing ventricle. *Nat Clin Pract Cardiovasc Med.* 2008;**5**(4):196–207. <https://doi.org/10.1038/ncpcardio.1130>.
- Pantano L. DESeqReport: report of DEG analysis. R package version 1.13.8. 2019. <https://doi.org/10.18129/B9.bioc.DESeqReport>.
- Paraskevopoulou S, Dennis AB, Weithoff G, Tiedemann R. Temperature-dependent life history and transcriptomic responses in heat-tolerant versus heat-sensitive *Brachionus* rotifers. *Sci Rep.* 2020;**10**(1):1–15. <https://doi.org/10.1038/s41598-020-70173-0>.
- Parrish JZ, Kim CC, Tang L, Bergquist S, Wang T, DeRisi JL, Jan LY, Jan YN, Davis GW. Krüppel mediates the selective rebalancing of ion channel expression. *Neuron* 2014;**82**(3):537–544. <https://doi.org/10.1016/j.neuron.2014.03.015>.
- Paul C, Kirschbaum F, Mamonekene V, Tiedemann R. Evidence for non-neutral evolution in a sodium channel gene in African weakly electric fish (*Campylomormyrus*, Mormyridae). *J Mol Evol.* 2016;**83**(1-2):61–77. <https://doi.org/10.1007/s00239-016-9754-8>.
- Paul C, Mamonekene V, Vater M, Feulner PGD, Engelmann J, Tiedemann R, Kirschbaum F. Comparative histology of the adult electric organ among four species of the genus *Campylomormyrus* (Teleostei: Mormyridae). *J Comp Physiol A Neuroethol Sens Neural Behav Physiol.* 2015;**201**(4):357–374. <https://doi.org/10.1007/s00359-015-0995-6>.
- Schrader LA, Birnbaum SG, Nadin BM, Ren Y, Bui D, Anderson AE, Sweatt JD. ERK/MAPK regulates the Kv4.2 potassium channel by direct phosphorylation of the pore-forming subunit. *Am J Physiol Cell Physiol.* 2006;**290**(3):852–861. <https://doi.org/10.1152/ajpcell.00358.2005>.
- Smith GT. Evolution and hormonal regulation of sex differences in the electrocommunication behavior of ghost knifefishes (Apteronotidae). *J Exp Biol.* 2013;**216**(13):2421–2433. <https://doi.org/10.1242/jeb.082933>.
- Soneson C, Love ML, Robinson MD. Differential analyses for RNA-seq: transcript-level estimates improve gene-level inferences. *F1000Res* 2015;**4**:1521. <https://doi.org/10.12688/f1000research.7563.1>.
- Stamboulian S, Choi JS, Ahn HS, Chang YW, Tyrrell L, Black JA, Waxman SG, Dib-Hajj SD. ERK1/2 mitogen-activated protein kinase phosphorylates sodium channel Na<sub>v</sub>1.7 and alters its gating properties. *J Neurosci.* 2010;**30**(5):1637–1647. <https://doi.org/10.1523/JNEUROSCI.4872-09.2010>.
- Stoddard PK, Markham MR. Signal cloaking by electric fish. *Bioscience* 2008;**58**(5):415–425. <https://doi.org/10.1641/B580508>.
- Swapna I, Ghezzi A, York JM, Markham MR, Halling DB, Lu Y, Gallant JR, Zakon HH. Electrostatic tuning of a potassium channel in electric fish. *Curr Biol.* 2018;**28**(13):2094–2102. <https://doi.org/10.1016/j.cub.2018.05.012>.
- Tiedemann R, Feulner PGD, Kirschbaum F. Electric organ discharge divergence promotes ecological speciation in sympatrically occurring African weakly electric fish (*Campylomormyrus*). In: Glaubrecht M, editor. *Evolution in action: case studies in adaptive radiation, speciation and the origin of biodiversity*. Berlin: Springer; 2010. p. 307–321.
- Traeger LL, Sabat G, Barrett-Wilt GA, Wells GB, Sussman MR. A tail of two voltages: proteomic comparison of the three electric organs of the electric eel. *Sci Adv.* 2017;**3**(7):e1700523. <https://doi.org/10.1126/sciadv.1700523>.
- Wang L, Shao Z, Chen S, Shi L, Li Z. A *SLC24A2* gene variant uncovered in pancreatic ductal adenocarcinoma by whole exome sequencing. *Tohoku J Exp Med.* 2017;**241**(4):287–295. <https://doi.org/10.1620/tjem.241.287>.
- Wang Y, Yang L. Genomic evidence for convergent molecular adaptation in electric fishes. *Genome Biol Evol.* 2021;**13**(3):1–11. <https://doi.org/10.1093/gbe/evab038>.
- Zakon HH. Adaptive evolution of voltage-gated sodium channels: the first 800 million years. *Proc Natl Acad Sci.* 2012;**109**(supplement\_1):10619–10625. <https://doi.org/10.1073/pnas.1201884109>.